Title: Milling time effect of Reactive Hydride Composites of NaF-NaH-MgB_2 investigated by *in situ* powder diffraction

Authors: Michael Heere[1], Magnus H. Sørby[1], Claudio Pistidda[2], Martin Dornheim[2], Bjørn C. Hauback[1,*]

[1]Physics Department, Institute for Energy Technology, NO-2027 Kjeller, Norway

[2]Institute of Materials Research, Materials Technology, Helmholtz-Zentrum Geesthacht, D-21502 Geesthacht, Germany

Key words: Hydrogen storage materials, *in situ* powder synchrotron diffraction, Reactive Hydride Composites

Abstract

Light metal complex borohydrides have high hydrogen storage capacities but suffer from drawbacks of slow hydrogen sorption kinetics, poor reversibility and high thermodynamic stability. The NaF+9NaH+5MgB_2 composite has a theoretical hydrogen capacity of 7.7 wt% H assuming the formation of 10$NaBH_{3.9}F_{0.1}$+5MgH_2. Hydrogenation and dehydrogenation properties as well as the effect of different ball milling times have been investigated. The *in situ* hydrogenation is faster in the composite ball milled for 87 h than the 5 h milled composite. A boron-rich phase with space group *Pa*-3, a = 7.4124(5) Å was formed during hydrogenation at 325 °C and 50 bar hydrogen for both short and long milling times. In the long milled composite the boron-rich phase disappeared after 3 h of hydrogenation, whereas it became a major phase in the short milled composite after 1.5 h of hydrogenation. $NaBH_4$ was formed at 206 °C. $NaMgH_{1-x}F_x$ was formed at 290 °C instead of the assumed MgH_2. The same phases formed at 268 °C and 325 °C, respectively, and only in minor amounts in the short milled composite. *Ex situ* hydrogenation in a Sieverts' type apparatus at the same temperature and hydrogen pressure conditions followed a different reaction pathway with formation of MgH_2 in addition to $NaBH_4$ and $NaMgH_{3-x}F_x$ ($0 \leq x \leq 1$). The measured hydrogen uptake was 6.0 wt% and 6.3 wt% for the long and short milled composites, respectively.

* Corresponding author
Phone: +47 97 40 88 44
Email: bjorn.hauback@ife.no

Introduction

Solid state hydrogen storage has the advantage over gaseous storage because of higher volumetric hydrogen storage capacities and lower pressures [1]. Reactive Hydride Composite (RHC) is an approach to tune the thermodynamics and kinetics of solid state hydrogen storage systems and make them more feasible for mobile application [2-4].

The stability of complex hydrides can be adjusted by anion substitution. Recently it was found that $Na_3AlH_{6-x}F_x$, formed from hydrogenation of NaF and Al, has a significant lower stability than Na_3AlH_6 [5, 6]. Substitution of hydrogen or a functional group with i.e. a halide, will change the bond strength, and the enthalpy of hydrogen sorption will be altered [7]. The hydrogenation properties of RHCs can thus be altered by partly substituting metal hydrides with metal halides i.e. fluorides, chlorides, bromides or iodides [8, 9].

It has been shown that a higher amount of hydrogen can be absorbed in CaH_2+MgB_2 when 25 mol% of the CaH_2 is substituted with CaF_2. The non-fluorinated system of CaH_2+MgB_2 has a theoretical hydrogen capacity of 8.3 wt%, but the experimental yield of absorbed hydrogen was only 3.5 wt%. The CaF_2-containing system absorbed twice as much hydrogen (7.0 wt%) with the same experimental conditions [10].

The theoretical hydrogen capacity of 2NaH+MgB_2 is 7.8 wt%, assuming that $2NaBH_4$ and MgH_2 are formed under hydrogenation. It has been found that this reaction is plagued by slow hydrogen sorption kinetics and by a low experimental hydrogen absorption capacity of only 3.8 wt% [11-14]. Pistidda et al. investigated this system and observed the formation of a boron-rich phase with space group *Pa*-3 and a = 7.319 Å forming during hydrogenation [13]. The proposed composition is $B_{48,}$ but the overall composition is still not clear, as the authors point out that inclusion in small amounts of other atoms like Mg and Na in the cubic lattice is possible [13].

This paper describes the adjustment of the thermodynamically stable 2NaH+MgB_2-system by substituting 10 mol% of the NaH with NaF forming NaF+9NaH+5MgB_2. Assuming a similar reaction pathway as above the theoretical hydrogen capacity would be 7.7 wt% for conversion for the starting reactions into $10NaBH_{3.9}F_{0.1}$+$5MgH_2$.

Experimental

Sample preparation: Commercially available powders of NaH (Sigma-Aldrich, >95%), MgB_2 (Sigma-Aldrich, >96%) and NaF (Sigma-Aldrich, >99%) were ball milled in a two-step process in a SPEX 8000D shaker mill for a total time of 87 and 5 h, respectively (long and short milled composite). The first step was to ball mill NaF-NaH in the molar ratio of 1:9 for about 60 h and 2.5 h, respectively. Then the products were ball milled with MgB_2 for 27 h and 2.5 h, respectively, in the molar ratio 2(NaF-NaH):1(MgB_2). Stainless steel vials with stainless steel-balls were used with a ball-to-powder ratio 10:1.

All sample manipulations were performed under argon atmosphere in a MBraun Unilab glove box with O_2/ H_2O levels kept below 1 ppm.

Hydrogenation: Hydrogenations were performed in an in-house manufactured Sieverts-type apparatus. The sample was gently hand grinded with mortar and pestle prior to loading it in the Sieverts apparatus to reactivate after being stored in the glove box. The hydrogen absorption was carried out with a temperature ramp of 5 °C min^{-1} from room temperature (RT) to 325 °C at 50 bar hydrogen pressure, followed by an isothermal step of 325 °C during a 41 h period.

Powder X-ray Diffraction (PXD): Data was collected using a Bruker AXS D8 Advance diffractometer in transmission mode, CuK_α λ = 1.5418 Å, fitted with a Göbbel mirror and a LynxEye™ 1D strip detector. The samples were measured over the scattering angle (2θ) from 10 ° to 90 ° with a step size Δ2θ of 0.02 °. The samples were contained within rotating boron-glass capillaries with an inner diameter of 0.5 mm. They were sealed used a 0.3 mm diameter boron-glass stick and glue.

***In situ* - Synchrotron Radiation Powder X-ray Diffraction (SR-PXD)** was conducted at the Swiss Norwegian Beam Lines, BM01A at ESRF in Grenoble, France [15]. Sapphire tubes (1.15 mm outer diameter, 0.8 mm inner diameter) connected to a Swagelok pressure cell were used. The high pressure gas rig and pressure cell are in-house manufactured. The *in situ* cycling experiments were conducted using a heating/cooling rate of 5 °C min^{-1} from RT to 325 °C (hot air blower) with hydrogen pressure of 50 bar for absorption and 1 bar hydrogen backpressure for desorption (510 °C). A Pilatus 2M detector was deployed and the sample-to-detector distance was 246 mm at a wavelength of 0.80645 Å or 0.784624 Å, respectively. The exposure

times were 30 s giving a resolution of 2.5 °C per diffraction pattern. The cell was rotated by 10 ° during each exposure to improve powder averaging.

All obtained raw images were transformed to 1D-powder patterns using the FIT2D program [16]. The wavelength and sample-detector distance were calibrated from a LaB_6 standard. Single crystal reflections from the sapphire tube were masked out manually in Fit2D. The Rietveld refinements were performed with GSAS and Expgui software [17, 18]. The peak shapes were modeled with a Thompson-Cox-Hastings pseudo-Voigt function with four refineable parameters (three Gaussian and one Lorentzian) [19]. The backgrounds were fitted with a Chebyshev polynomial with up to 36 terms.

Results and discussion

Ball milled samples

Before the *in situ* hydrogenation, the samples were measured by SR-PXD in their “as-milled” state at RT. The width of the Bragg peaks is different after ball milling for 87 and 5 h, respectively (see Fig. S1 and S2 in Supporting information). In the long milled sample the Bragg peaks from the initial compounds NaH and NaF were replaced with broad peaks from a single fcc phase; FWHM = 0.228 ° at 2θ = 16.542 °. This corresponds to a particle size of 18 nm calculated using the Scherrer formula [20]. The lattice parameter of the face-centered cubic phase was a = 4.86529(8) Å. This lattice parameter is slightly smaller due to partial fluorine substitution (NaF a = 4.78 Å [21]) compared to that reported for NaH (a = 4.89 Å [22]). From Rietveld refinements the composition of this phase is proposed to be $NaH_{1-x}F_x$ with x = 0.099(1), and thus confirming the formation of a single solid solution phase. In contrast, in the short milled sample, the Bragg peaks of F-substituted NaH and NaF were distinguishable after ball milling with FWHM = 0.128 ° for NaH at 2θ = 16.542 °, corresponding to a calculated particle size of 32 nm for NaH.

From Rietveld refinements with the SR-PXD data at RT for the 87 h milled sample (Fig. S1 in Supporting information), the fractions of the reactants were 44.5(2) wt% MgB_2, 51.2(3) wt% $NaH_{1-x}F_x$ with x = 0.099(1) and 4.3(1) wt% Fe. Fe was a contamination from the ball mill. These values are in good agreement with the nominal composition, 47 wt% MgB_2, 44 wt% NaH and 8 wt% NaF (corresponding to 52 wt% $NaH_{0.9}F_{0.1}$).

The 5 h milled composite shows sharp Bragg peaks after ball milling, and all reactants can be identified (Fig. S2 in Supporting information). The refined phase composition was 37.0(6) wt% MgB_2, 59.6(6) wt% $NaH_{1-x}F_x$ with x = 0.078(1) and 2.9(3) wt% for NaF. The incomplete incorporation of F^- in the solid solution $NaH_{1-x}F_x$ is reflected in the smaller unit cell axis of a = 4.8589(8) Å, compared 4.86529(8) Å in the 87 h milled sample. 0.5(1) wt% Fe is present as a contamination. The refined phase fractions are in agreement with the nominal composition.

Hydrogenation of long milled NaF+9NaH+5MgB_2

The *in situ* SR-PXD hydrogenation measurements were performed at 50 bar of H_2 heating the sample from RT to 325 °C with a heating rate of 5 °C min^{-1} and followed by 5 h isotherm at 325 °C. The first hydrogenation product, $NaBH_4$, was observed at 206 °C (green curve in Fig. 1a). $NaMgH_{3-x}F_x$ started to form at 290 °C (red curve in Fig. 1a). This compound is more stable than MgH_2 and therefore the favored product [23, 24]. The intensity of the $NaH_{1-x}F_x$ Bragg peak at 16.5 ° was decreasing and becoming narrower when the $NaMgH_{3-x}F_x$ was formed, suggesting that fluorine from $NaH_{1-x}F_x$ was incorporated into $NaMgH_3$ structure. This was also evident from the increase of lattice parameters to a = 5.47345(16), b = 7.7157(2), c = 5.41953(15) compared to a = 5.4596(2), b = 7.6982(4), c = 5.4086(2) for $NaMgH_3$ at RT [25]. This change is about two orders of magnitude more than expected from thermal expansion. The Rietveld refinement (Fig. 3a) indicates $NaMgH_{3-x}F_x$ with x = 0.83(4). Both phases were present after 5 h of isothermal hydrogen absorption at 325 °C (Fig. S3 in Supporting information). The two main phases were $NaBH_4$, 41.5(2) wt%, and $NaMgH_{3-x}F_x$ with x=0.848(3), 24.5(2) wt%, whereas the amounts of MgB_2 and $NaH_{1-x}F_x$ decreased from 44.5(2) wt% and 51.2(3) wt% with x = 0.099(1) after ball milling to 17.8(1) wt% and 6.9(1) wt% with x = 0.074(4), respectively. This shows that the hydrogenation was not completed. After reaching 325 °C at 50 bar hydrogen, SR-PXD data were collected for 5 h under isothermal conditions (Fig. 1a). A phase similar to the earlier reported boron-rich phase ("B_{48}") [13] started to form after 6 min at 325 °C. This is an intermediate phase as it disappeared after 135 min at the isothermal condition. The *ex situ* hydrogenation data (Fig. 2c) indicates that 5 h of hydrogenation should lead to the absorption of approximately 5 wt% H. The reaction temperatures are lower than earlier reported in ref [26], where $NaMgH_3$ and $NaBH_4$ were formed at 330 °C and 380 °C, respectively. Our observation that $NaBH_4$ is formed prior to $NaMgH_{3-x}F_x$ indicates a changed reaction path because of incorporation of fluorine into the structure.

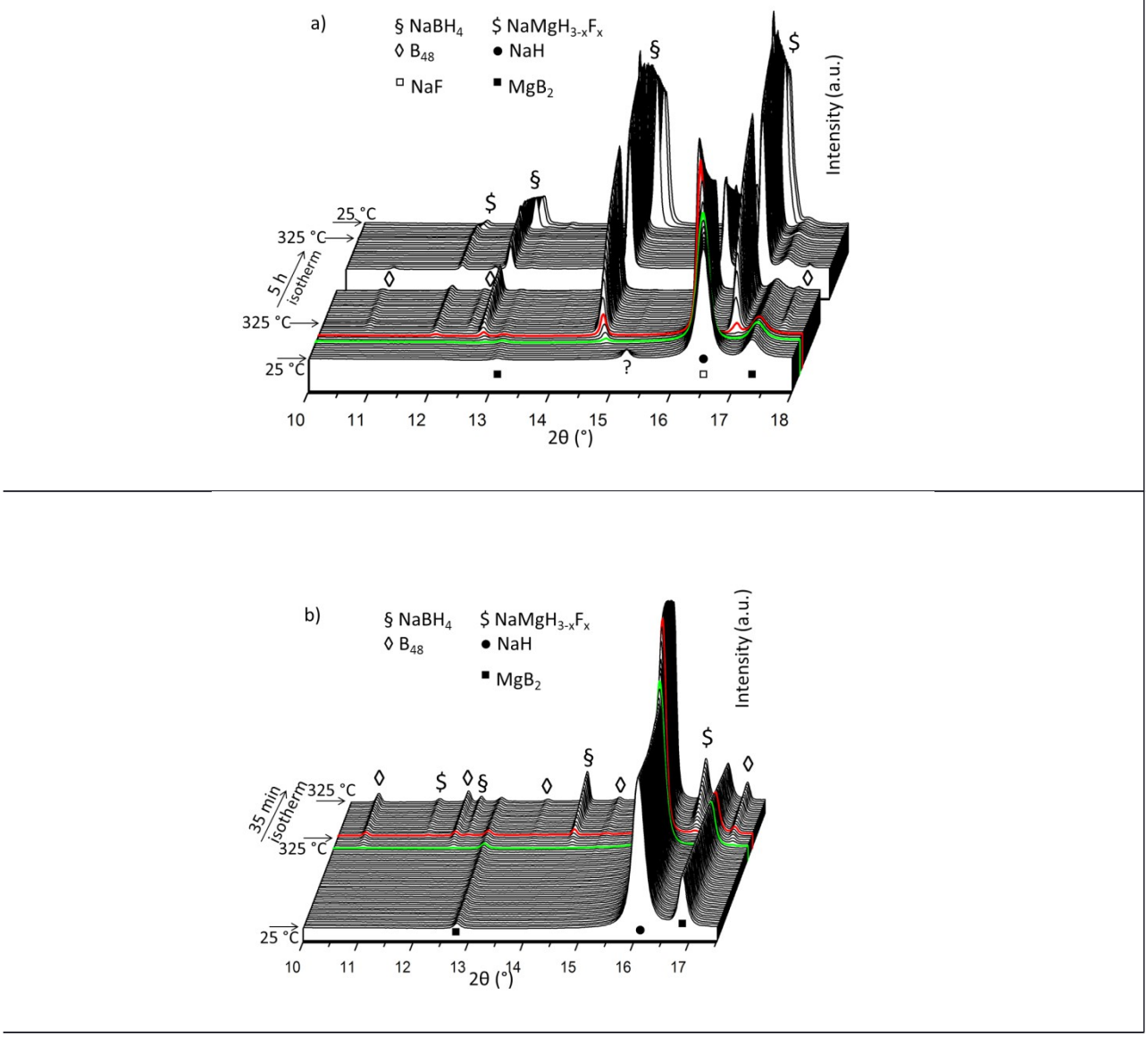

Fig. 1 - *In situ* SR-PXD data from the absorption process of NaH + 9 NaF + 5 MgB_2 between 25 °C and 325 °C plus a 5 h isotherm (Fig. 1a) and 35 min isotherm (Fig. 1b) at 50 bar H_2 are shown. (a) long milled NaF+9NaH+5MgB_2, Green Curve (front) showing the formation of $NaBH_4$ at 206 °C and red curve (back) the formation of $NaMgH_{3-x}F_x$ at 290 °C. The intermediate boron-rich phase ("B_{48}") is also shown. The gap in the data in the isothermal step is due to an accidental interruption of the measurement. λ = 0.80645 Å. (b) short milled NaF+9NaH+5MgB_2; Green Curve (front) showing the formation of $NaBH_4$ and "B_{48}" at 268 °C. Red curve (back) the formation of $NaMgH_{3-x}F_x$ after 7 min at 325 °C. λ = 0.784624 Å.

The hydrogenation was repeated *ex situ* in a Sieverts' apparatus under the same conditions, but prolonging the isothermal treatments at 325 °C to 41 h. PXD of the hydrogenation product confirms the following reaction:

$$10NaH_{0.9}F_{0.1(s)}+5MgB_{2(s)}+15.5H_{2(g)} \rightarrow 9NaBH_{4(s)}+NaMgH_2F_{(s)}+MgH_{2(s)}+\text{unknown phase} \quad (1)$$

The Rietveld refinement with the PXD data is shown in Fig. 2a. The observed weight fractions for identified phases of 78.4(2) wt% $NaBH_4$, 15.1(3) wt% $NaMgH_{3-x}F_x$ with x = 0.35(13) and 6.6(3) wt% MgH_2 are in good agreement with the theoretical fractions from eq. 1 for identified phases as stated above of 78.3 wt%, 15.7 wt% and 6.0 wt%, respectively. In addition there are Bragg peaks from one or more unidentified phases which account for the remaining 3Mg + 1B, corresponding to 16.1 wt% of the sample.

The theoretical hydrogen capacity from eq. 1 is 6.0 wt% which is equal to the observed value from the Sieverts' measurement. The formation of MgH_2 has been proposed not to be favorable compared to $NaMgH_3$ [23, 24]. However, the presence of MgH_2 in our *ex situ* data is in agreement with other experimental data [12, 27].

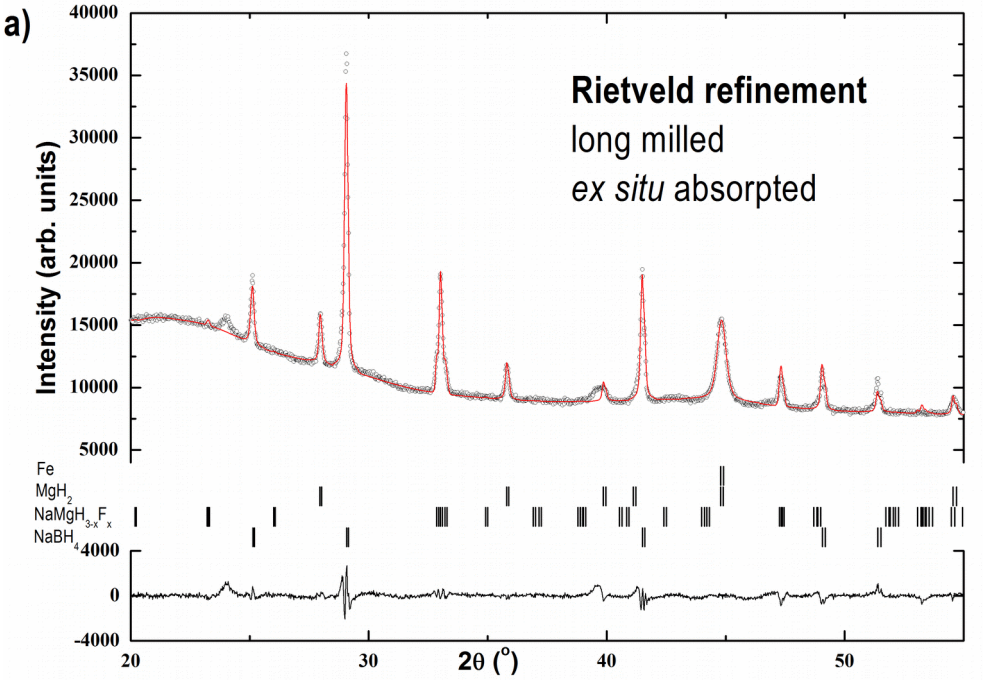
a)
Rietveld refinement
long milled
ex situ absorpted
Intensity (arb. units)
Fe
MgH2
NaMgH3-xFx
NaBH4
2θ (°)

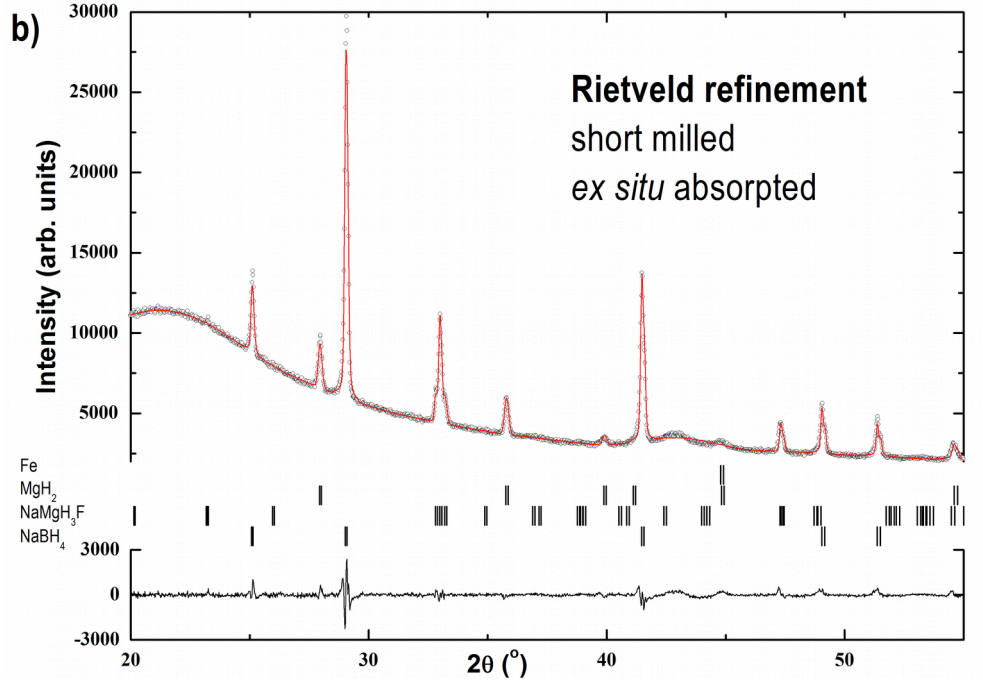
b)
Rietveld refinement
short milled
ex situ absorpted
Intensity (arb. units)
Fe
MgH2
NaMgH3F
NaBH4
2θ (°)

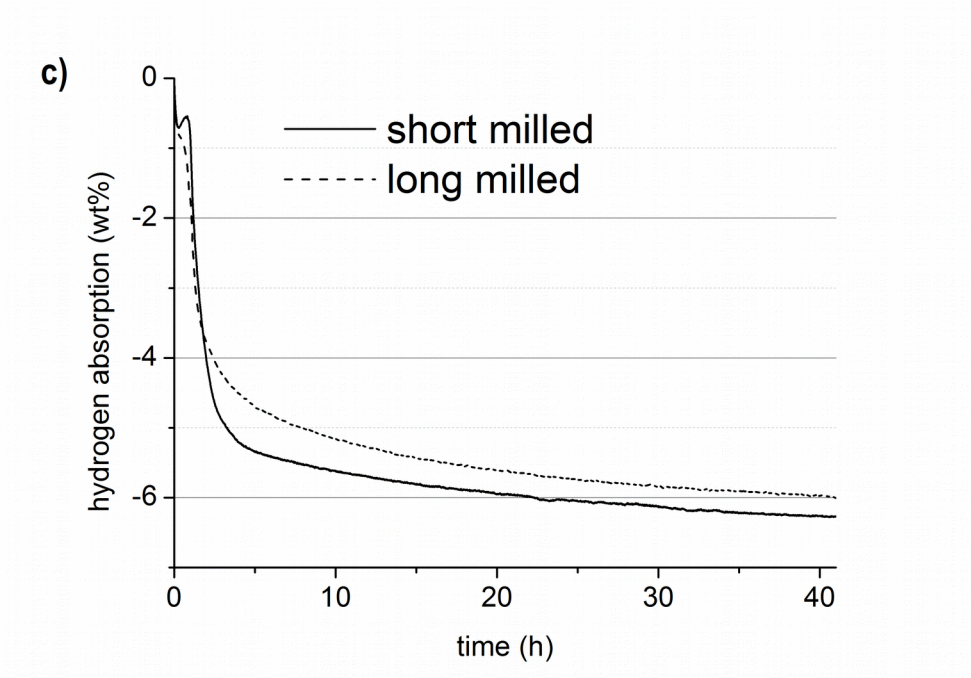

Fig. 2 - (a) Rietveld refinement to the *ex situ* PXD data after hydrogenation in the Sieverts' apparatus at RT showing experimental (circles) and calculated (red line) patterns, and a difference plot (below) for the long milled NaF+9NaH+5MgB_2 after 41 h at 325°C. Vertical ticks mark the Bragg peak positions for (from top): Fe, MgH_2 (6.6(3) wt%), $NaMgH_{3-x}F_x$ (15.1(3) wt%, x = 0.35(13)) and $NaBH_4$ (78.4(2) wt%). R_{wp} = 5.48 % and (b) Rietveld refinement for the short milled NaF+9NaH+5MgB_2 after 41 h at 325°C. Vertical ticks mark the Bragg peak positions for (from top): Fe, MgH_2 (9.5(2) wt%), $NaMgH_3$ (8.5(1) wt%) and $NaBH_4$ (82.1(2) wt%). R_{wp} = 2.58 %; (c) *ex situ* hydrogenation of NaF+9NaH+5MgB_2 at 325 °C and 50 bar H_2 pressure. The total hydrogen contents achieved for short milled and long milled system are 6.3 wt% and 6.0 wt%, respectively.

Hydrogenation of short milled NaF+9NaH+5MgB_2

During the *in situ* hydrogenation with heating rate 5 C min^{-1} and 50 bar H_2 pressure of the short milled sample the boron-rich phase ("B_{48}") was already formed at 268 °C during heating, and minor Bragg peaks from $NaBH_4$ appeared simultaneously (Fig. 1b, green curve). Weak Bragg peaks from $NaMgH_{3-x}F_x$ was first observed in the isothermal regime after 9 min at 325 °C (Fig. 1b, red curve). This is in contrast to what was observed in the case of the long milled composite where $NaBH_4$ and $NaMgH_{3-x}F_x$ appeared first and "B_{48}" was an intermediate phase. After 35 min isothermal hydrogenation at 325 °C, "B_{48}" became a major hydrogenation product together with $NaMgH_{3-x}F_x$. We assume the presence of the "B_{48}" phase is the main reason why $NaBH_4$ and $NaMgH_{3-x}F_x$ are formed at higher temperatures compared to the long milled composite.

The *ex situ* hydrogenation data (Fig. 2c) at 50 bar hydrogen and 325 °C for the short milled sample gives a hydrogen uptake of 3 wt% after 1.5 h hydrogenation (1h heating + 35 min isotherm). This is surprising, as the *in situ* hydrogenation products in Fig. 3a, $NaBH_4$ and $NaMgH_{3-x}F_x$, are only minor phases with refined weight fractions of 4.2(1) wt% and 4.9(1) wt%, respectively, after the same hydrogenation time. If these two phases with the observed amounts were the only hydrogenation products, it would correspond to a hydrogen uptake of only 0.3 wt % H for the composite. Hence, it seems likely that the "B_{48}" phase is a hydrogenation product that contains most of the absorbed hydrogen. Another possible explanation is that non-crystalline phases absorb hydrogen and form non-crystalline products, although this seems less likely as no appreciable diffuse scattering is observed in the SR-PXD data.

The boron-rich "B_{48}" phase was observed in both composites. Rietveld refinements with the structure model from ref. [13] yielded unphysically high temperature factors and thus a large overestimation of its phase fraction. This was taken as an indication that the structure model is not complete, as already suggested by Pistidda et al. [13]. Thus the phase was fitted with Le Bail (i.e. structureless) refinements, and is not accounted for the reported phase compositions of the samples. During hydrogenation this phase was reported to form prior to $NaMgH_3$ [13], in agreement with our observation for the short-milled composite. In contrast "B_{48}" was formed after $NaMgH_{3-x}F_x$ during the reaction in the long milled composite, and it disappeared after 3 h hydrogenation at 325 °C.

During the *in situ* hydrogenation at 50 bar of the short milled sample a pressure reduction was observed during the formation of "B_{48}", which support the assumption that this phase contained hydrogen in addition to boron. It is supported by the *ex situ* Sieverts' data (Fig. 2c), which showed a rapid hydrogen uptake during the first 1.5 h. According to the *in situ* SR-PXD data "B_{48}" was formed during the first 1.5 h of hydrogenation. Preparation of an isotope substituted sample (^{11}B and D) for powder neutron diffraction is planned to clarify the nature of "B_{48}".

The repeated *ex situ* hydrogenation in the Sieverts' apparatus under the same conditions, with an isothermal treatment at 325 °C for 41 h, leads to the assumption that the reaction pathway in the short milled composite is slightly different. The following reaction eq. 2 is proposed based on the hydrogenation products shown and refined with the data in Fig. 2b:

$$9NaH_{(s)} + NaF_{(s)} + 5MgB_{2(s)} + 16.875H_{2(g)} \rightarrow 9.25NaBH_{4(s)} + 0.75NaMgH_{3(s)} + 1.75MgH_{2(s)} + \text{non-crystalline} \quad (2)$$

The refined weight fractions for identified phases of 82.1(2) wt% $NaBH_4$, 8.5(1) wt% $NaMgH_3$ and 9.5(2) wt% MgH_2 are in agreement with the theoretical weight fractions from eq. 2 for identified phases as stated above of 80.7 wt%, 8.7 wt% and 10.6 wt%, respectively. The incorporation of fluorine into the lattice of $NaMgH_3$ was not observed. The remaining amounts of 2.5Mg, 1F and 0.75B are assumed to be in amorphous and/or nanocrystalline phase since no unidentified phases are observed (non-crystalline = 16.8 wt%). The theoretical hydrogen capacity from eq. 2 is 6.5 wt% if the non-crystalline phase is not hydrogen-containing. This amount coincides with the observed value of 6.3 wt% from the Sieverts' measurement. The formation of MgH_2 has been proposed not to be favorable compared to $NaMgH_3$ [23, 24]. However, the presence of MgH_2 in our *ex situ* data is in agreement with other experimental data [12, 27].

The amount of absorbed hydrogen is more than 65 % higher than reported earlier at the same conditions and time, 3.8 wt%, for a fluorine-free composite [14]. Moreover, the kinetics are greatly improved. In the work by Pistidda et al. it took 2 h to obtain 2 wt% H and 63 h to reach 6.2 wt% at 25 bar. In our experiment at 50 bar, 4 wt% was absorbed after 2 h and 6.3 wt% after 41 h at 325 °C.

Rietveld refinements with SR-PXD data of *in situ* hydrogenation for the short- and long-milled samples with a heating rate 5 °C min^{-1} from RT to 325 °C and 35 min or 55 min isotherm at 325 °C, respectively, are shown in Fig. 3a and b. The amounts of the hydrogenation products are larger in the long milled composite with 26.6(3) wt% $NaBH_4$ and $NaMgH_{3-x}F_x$ 12.2(1) wt%, compared to 4.2(1) and 4.9(1) wt%, respectively, in the short-milled composite. "B_{48}" is fitted with Le Bail refinement (see above). The differences between the composites could be explained by the different particle sizes obtained by the different milling times.

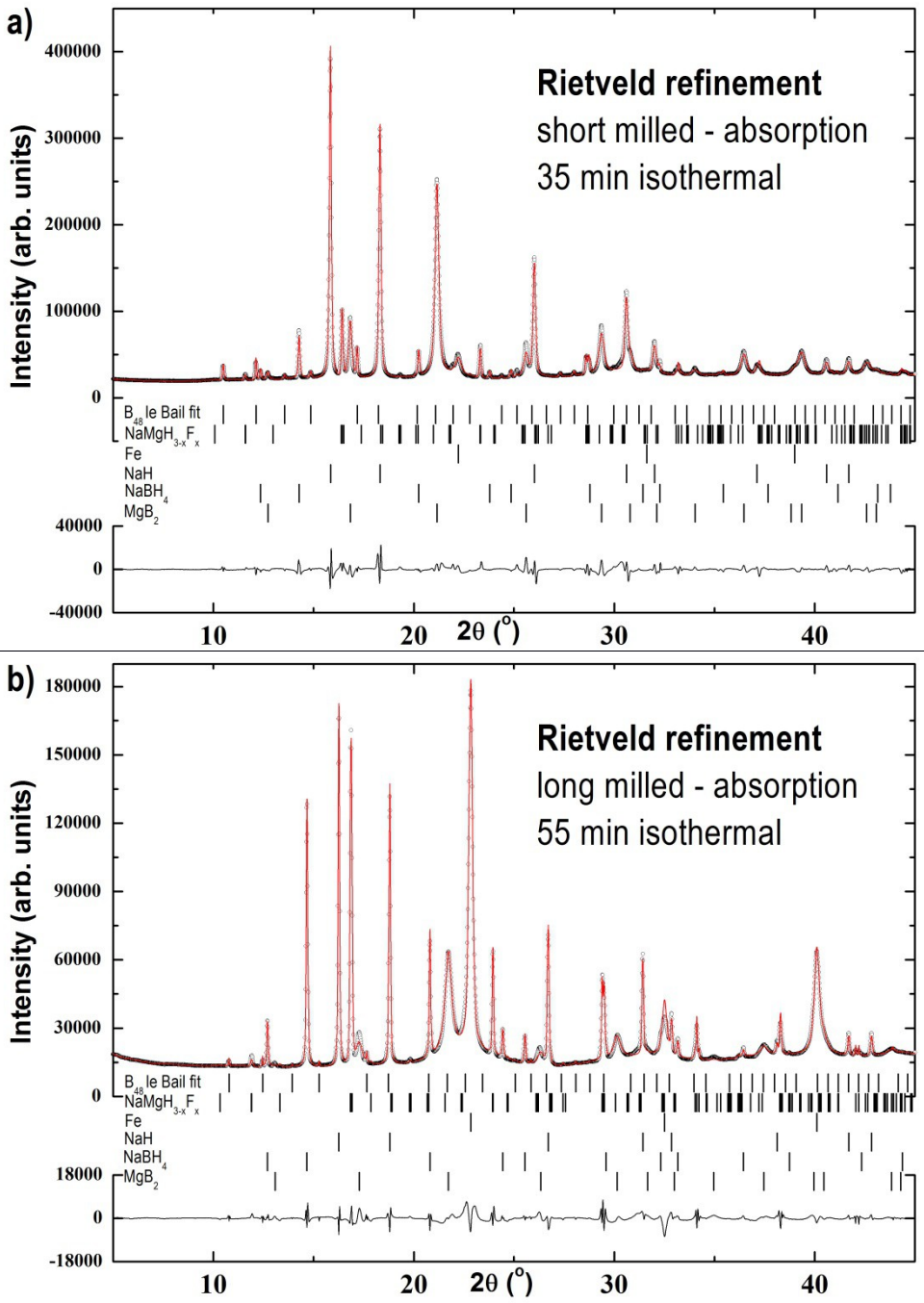

Fig. 3 - Rietveld refinement plot from SR-PXD patterns at 325 °C showing experimental (circles) and calculated (red line) patterns, and a difference plot (below) for the (a) short milled NaF+9NaH+5MgB_2 after 35 min at 325°C. Vertical ticks mark the Bragg peak positions for (from top): "B_{48}" (Le Bail fit), $NaMgH_{3-x}F_x$ (4.9(1) wt%, x = 0.81(19)), Fe (1.2(1) wt%), NaH (43.4(1) wt%), $NaBH_4$ (4.2(1) wt%) and MgB_2 (46.3(1) wt%); R_{wp} = 4.68%; λ = 0.784624 Å; and (b) long milled NaF+9NaH+5MgB_2 after 55 min at 325°C Vertical ticks mark the Bragg peak positions for (from top): "B_{48}" (Le Bail fit), $NaMgH_{3-x}F_x$ (12.2(1) wt%, x = 0.83(4)), Fe (6.9(1) wt%), NaH (18.0(1) wt%), $NaBH_4$ (26.6(3) wt%) and MgB_2 (36.4(2) wt%); R_{wp} = 4.2%, λ = 0.80645 Å.

Dehydrogenation of long milled NaF+9NaH+5MgB_2

After 5 h of *in situ* hydrogenation followed by cooling to RT under 50 bar H_2, the long milled sample was decomposed *in situ*. From RT to 200 °C the sample was heated with 20 °C min^{-1}, then further to 510 °C with 5 °C min^{-1} and finished with an isothermal step for 1 h at 510 °C. 1 bar hydrogen backpressure was applied at the start of the dehydrogenation process. The desorption shown in Fig. 4 is characterized by two main steps. Step 1 is from RT to approx. 400 °C and step 2 from 400 °C to 510 °C plus 1 h of isothermal treatment.

Step 1: Both NaH and $NaBH_4$ started to disappear at 366 °C and disappeared completely at 378 and 402 °C, respectively. Diffuse scattering is increased as the Bragg peaks from these phases are decreased in intensity, probably due to a molten NaH:$NaBH_4$ eutectic. This is in agreement with earlier results showing a molten mixture of NaH and $NaBH_4$ that is present at 383 °C for 5 and 50 bar H_2 [28]. This is below the melting points of both NaH at 400 °C [29] and $NaBH_4$ at 505 °C [30].

Step 2: Mg appeared at 391 °C and disappeared at 507 °C. The amount of $NaMgH_{3-x}F_x$ is decreasing between 385 and 450 °C. From 450 °C it is present as a minority phase and the amount did not decrease further. The Bragg peaks from Mg decreased from 480 °C while those from MgB_2 increased in intensity. At 507 °C the remaining Bragg peaks from Mg and the diffuse scattering from the NaH:$NaBH_4$ melt disappeared abruptly with a corresponding increase in the Bragg peak intensities from MgB_2. FeB was observed at 450 °C and the intensity in these Bragg peaks increased until the iron contaminant had been consumed after 15 min at 510 °C. Because of the FeB formation in the long milled sample the data in Fig. 4 cannot be directly compared with the short milled sample.

After 50 min at 510 °C the amounts of MgB_2 and $NaMgH_{3-x}F_x$ were not changing any further. $NaMgH_3$ is reported to be stable up to 500 °C at 10 bar H_2 [24]. The presence of $NaMgH_{3-x}F_x$ as a minority phase at 510 °C at 1 bar H_2 indicates a stabilizing effect by fluorine substitution.

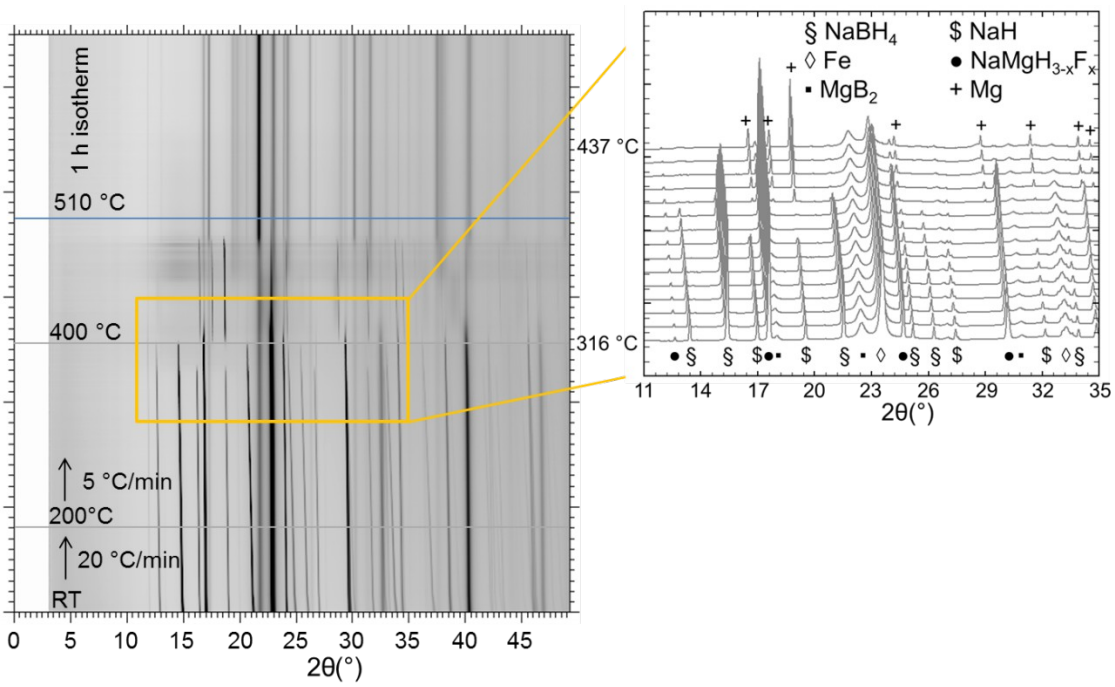

Fig. 4 - *In situ* SR-PXD data of 2 step desorption process in long milled NaH + 9NaF + $5MgB_2$. Heating from RT to 200 °C with 20 °C min^{-1}, 200 °C to 510 °C with 5 °C min^{-1} and isothermal step for 1 h at 510 °C. A darker color corresponds to a higher diffraction intensity. Inset showing Bragg peaks from a selected area between 316 °C and 437 °C, λ = 0.80645 Å.

De- and re-hydrogenation of short milled NaF+9NaH+5MgB_2

The *in situ* decomposition SR-PXD measurement of the short milled sample followed the *in situ* hydrogenation described above by lowering the pressure to 1 bar and heating from 325 to 510 °C at 5 °C min^{-1}. A 1 h isothermal step was applied at the end of the heating ramp. The SR-PXD data are shown in Fig. 5a. Bragg peaks from $NaBH_4$ and "B_{48}" decreased from 325 °C and disappeared at 353 °C (grey line in Fig. 5a). The Bragg peaks corresponding to $NaMgH_{3-x}F_x$ were decreasing along with those from $NaH_{1-x}F_x$ until the peaks from both phases disappeared at 491 °C. This is above the melting point of NaH (400 °C [29]), thus indicating a stabilizing effect of fluorine substitution. After the Bragg peaks from $NaH_{1-x}F_x$ disappeared, diffuse scattering appeared, indicating melting of $NaH_{1-x}F_x$. The molten $NaH_{1-x}F_x$ and Mg in a nanocrystalline state were probably responsible for the reappearance of weak Bragg peaks from $NaMgH_{3-x}F_x$. This process stopped when Bragg peaks of Mg appeared at 495 °C. After 60 min at 510 °C the intensities of the Bragg peaks from Mg, MgB_2 and $NaMgH_{3-x}F_x$ did not change any

further. The stabilizing effect of the fluorine substitution in $NaMgH_{3-x}F_x$ and $NaH_{1-x}F_x$ is again evident.

The *in situ* re-hydrogenation started with cooling from 510 to 325 °C with a rate of -5 °C min^{-1} (1 bar H_2 backpressure) and at 325 °C 50 bar of hydrogen was introduced (blue line in Fig. 5b). Fig. 5b shows that $NaBH_4$ crystallized at 368 °C (orange line) before hydrogen pressure was increased (blue line). The yield was 52.5(2) wt% (Fig. S4 in Supporting information). Since $NaBH_4$ was only present in a minor amount after the first hydrogenation (Fig. 3a), it is clear that $NaBH_4$ must have been formed in a hydrogenation process in the melt under 1 bar H_2. This is in agreement with earlier observation that a higher amount of $NaBH_4$ is appearing for hydrogenation at rather low pressures of 5 bar hydrogen compared to higher pressures of 25 or 50 bar hydrogen [14]. Our recrystallization temperature for $NaBH_4$, 368 °C, is in excellent agreement with the literature value of 363 °C [14]. Both "B_{48}" and $NaBH_4$ appeared at 268 °C during the first *in situ* hydrogenation, and disappeared at the same temperature during *in situ* desorption. Thus it can be suggested that both phases are formed and consumed in the same reactions.

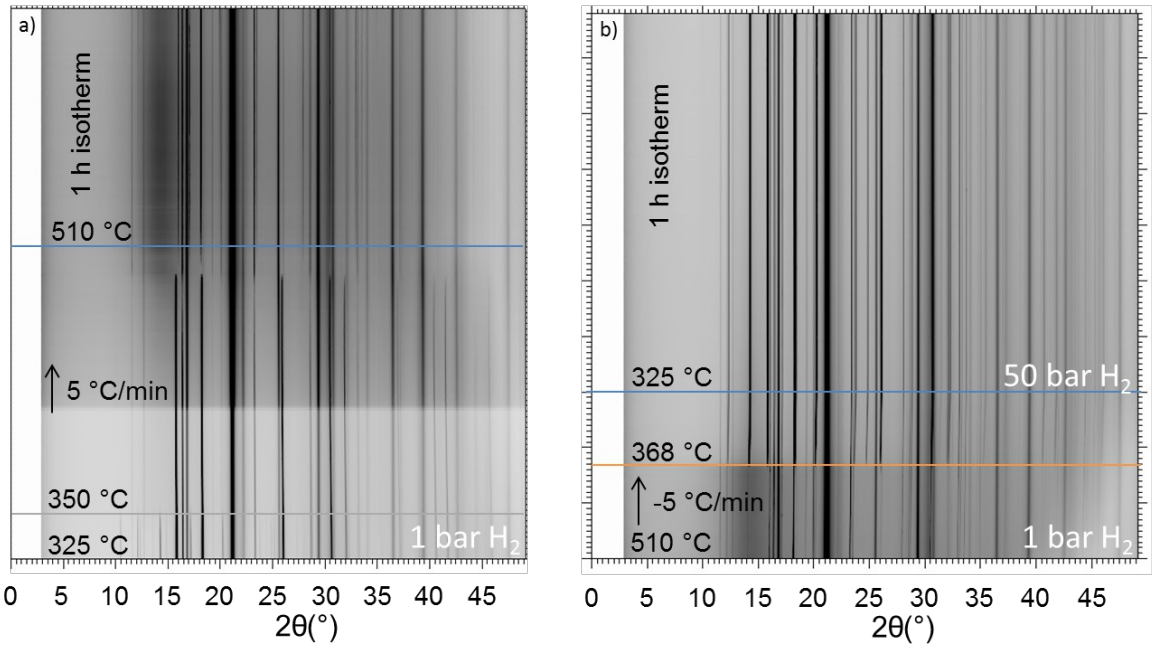

Fig.5 - (a) *In situ* decomposition of short milled $NaF+9NaH+5MgB_2$. Heating ramp from 325 to 510 °C at 5 °C min^{-1} and an isothermal step of 1 hour at 1 bar hydrogen backpressure. (b) *in situ r*e-hydrogenation of short milled $NaF+9NaH+5MgB_2$. Cooling ramp from 510 to 325 °C at -5 °C min^{-1} at 1 bar hydrogen backpressure and 50 bar hydrogen applied at 325 °C. A darker color corresponds to a higher diffraction intensity.

Conclusions and Outlook

The hydrogen sorption properties of the $2NaH+MgB_2$-system was enhanced by adding 10 mol% NaF. The theoretical hydrogen capacity of the investigated systems $NaF+9NaH+5MgB_2$ is 7.7 wt % with the formation of $10NaBH_{3.9}F_{0.1} + 5MgH_2$. A different reaction pathway resulting in the hydrogenation products $NaBH_4$, MgH_2 and $NaMgH_{3-x}F_x$ ($0 \leq x \leq 1$) gives an *ex situ* measured hydrogen capacity of 6.0 wt% for the long milled composite (Sieverts' apparatus). *Ex situ* hydrogenation of the short milled composite at the same conditions resulted in a hydrogen uptake of 6.3 wt% H, with a slightly different reaction pathway as the long milled composite.

The thermodynamics of this system have been modified compared to the non-fluorinated systems investigated by Nwakwuo et al. [26] and Pistidda et al [14], especially when taking into consideration that the formation of $NaBH_4$ which is reported to start at 380 °C is decreased to 206 °C and 268 °C in our long milled sample and short milled sample, respectively.

The boron-rich phase "B_{48}" appeared in both samples. In the short milled sample it constitutes a major crystalline phase after 1.5 h, whereas it disappeared in the long milled sample after 3 h of hydrogenation. The "B_{48}" phase was not found after *in situ* re-hydrogenation in the short milled sample, as $NaBH_4$ is formed instead as the major phase with a fraction of 52.5(2) wt% at low pressures of approx. 1 bar H_2.

The composition of the boron-rich "B_{48}" is still not clear, but there are strong indications that it contains hydrogen in addition to boron. Neutron diffraction measurements will be conducted to clarify the nature of this phase.

Acknowledgments

The research leading to these results has received funding from the People Program (Marie Curie Actions) of the European Union's Seventh Framework Program FP7/2007-2013/ under REA grant agreement n° 607040 (Marie Curie ITN ECOSTORE) is thankfully acknowledged. The authors acknowledge the skillful assistance from the staff of the Swiss-Norwegian Beamline, at the European Synchrotron Radiation Facility, Grenoble, France.

References

[1] Schlapbach, L. and A. Züttel, *Hydrogen-storage materials for mobile applications.* Nature, 2001. **414**(6861): p. 353-358.

[2] Dornheim, M., S. Doppiu, G. Barkhordarian, U. Bösenberg, T. Klassen, O. Gutfleisch, and R. Bormann, *Hydrogen storage in magnesium-based hydrides and hydride composites.* Scripta Materialia, 2007. **56**(10): p. 841-846.

[3] Vajo, J.J., S.L. Skeith, and F. Mertens, *Reversible storage of hydrogen in destabilized LiBH4.* The Journal of Physical Chemistry B, 2005. **109**(9): p. 3719-3722.

[4] Chen, P., Z. Xiong, J. Luo, J. Lin, and K.L. Tan, *Interaction of hydrogen with metal nitrides and imides.* Nature, 2002. **420**(6913): p. 302-304.

[5] Brinks, H.W., A. Fossdal, and B.C. Hauback, *Adjustment of the stability of complex hydrides by anion substitution.* Journal of Physical Chemistry C, 2008. **112**(14): p. 5658-5661.

[6] Eigen, N., U. Bösenberg, J.B. von Colbe, T.R. Jensen, Y. Cerenius, M. Dornheim, T. Klassen, and R. Bormann, *Reversible hydrogen storage in NaF-Al composites.* Journal of Alloys and Compounds, 2009. **477**(1-2): p. 76-80.

[7] Taube, K. *FLYHY - Fluorine Substituted High Capacity Hydrides for Hydrogen Storage at Low Working Temperatures - Summary of 1st Reporting Period*. 03.08.2011]; Available from: http://www.flyhy.eu/Downloads/FLYHY%20Publishable%20Summary%202009-2010%20Web.pdf.

[8] Kim, J.-H., J.-H. Shim, and Y.W. Cho, *On the reversibility of hydrogen storage in Ti- and Nb-catalyzed Ca(BH4)2.* Journal of Power Sources, 2008. **181**(1): p. 140-143.

[9] Wang, P., X.D. Kang, and H.M. Cheng, *Improved Hydrogen Storage of TiF3-Doped NaAlH4.* ChemPhysChem, 2005. **6**(12): p. 2488-2491.

[10] Suarez Alcantara, K., U. Bösenberg, O. Zavorotynska, J. Bellosta von Colbe, K. Taube, M. Baricco, T. Klassen, and M. Dornheim, *Sorption and desorption properties of a CaH2/MgB2/CaF2 reactive hydride composite as potential hydrogen storage material.* Journal of Solid State Chemistry, 2011. **184**(11): p. 3104-3109.

[11] Garroni, S., C. Pistidda, M. Brunelli, G.B.M. Vaughan, S. Surinach, and M.D. Baro, Scripta Mater. 60, 2009: p. 1129.

[12] Mao, J.F., X.B. Yu, Z.P. Guo, H.K. Liu, Z. Wu, and J. Ni, *Enhanced hydrogen storage performances of NaBH4–MgH2 system.* Journal of Alloys and Compounds, 2009. **479**(1–2): p. 619-623.

[13] Pistidda, C., E. Napolitano, D. Pottmaier, M. Dornheim, T. Klassen, M. Baricco, and S. Enzo, *Structural study of a new B-rich phase obtained by partial hydrogenation of 2NaH+ MgB 2.* international journal of hydrogen energy, 2013. **38**(25): p. 10479-10484.

[14] Pistidda, C., S. Garroni, C.B. Minella, F. Dolci, T.R. Jensen, P. Nolis, U. Bösenberg, Y. Cerenius, W. Lohstroh, M. Fichtner, M.D. Baró, R. Bormann, and M. Dornheim, *Pressure Effect on the 2NaH + MgB2 Hydrogen Absorption Reaction.* The Journal of Physical Chemistry C, 2010. **114**(49): p. 21816-21823.

[15] Dyadkin, V., P. Pattison, V. Dmitriev, and D. Chernyshov, *A new multipurpose diffractometer PILATUS@SNBL.* Journal of Synchrotron Radiation, 2016. **23**(3).

[16] Hammersley, A., *FIT2D: An introduction and overview, ESRF Int.* Rep., ESRF97HA02T, 1997.

[17] Larson, A. and R. Von Dreele, *General Structure Analysis System (GSAS); Report LAUR 86-748; Los Alamos National Laboratory: Los Alamos, NM, 2000.* There is no corresponding record for this reference.

[18] Toby, B.H., *EXPGUI, a graphical user interface for GSAS.* Journal of applied crystallography, 2001. **34**(2): p. 210-213.

[19] Thompson, P., D. Cox, and J. Hastings, *Rietveld refinement of Debye–Scherrer synchrotron X-ray data from Al2O3*. Journal of Applied Crystallography, 1987. **20**(2): p. 79-83.
[20] Scherrer, P., *Nachrichten von der Gesellschaft der Wissenschaften zu Göttingen, Mathematisch-Physikalische Klasse*. 1918.
[21] Bragg, W., *Crystal structure*. Nature, 1920. **105**: p. 646-648.
[22] Shull, C.G., E.O. Wollan, G.A. Morton, and W.L. Davidson, *Neutron Diffraction Studies of NaH and NaD*. Physical Review, 1948. **73**(8): p. 842-847.
[23] Wu, H., W. Zhou, T.J. Udovic, J.J. Rush, and T. Yildirim, Chem. Mater. 20 2008: p. 2335.
[24] Ikeda, K., Y. Kogure, Y. Nakamori, and S. Orimo, *Reversible hydriding and dehydriding reactions of perovskite-type hydride NaMgH3.* Scripta Materialia, 2005. **53**(3): p. 319-322.
[25] Ikeda, K., S. Kato, Y. Shinzato, N. Okuda, Y. Nakamori, A. Kitano, H. Yukawa, M. Morinaga, and S. Orimo, *Thermodynamical stability and electronic structure of a perovskite-type hydride, NaMgH 3*. Journal of Alloys and Compounds, 2007. **446**: p. 162-165.
[26] Nwakwuo, C.C., C. Pistidda, M. Dornheim, J.L. Hutchison, and J.M. Sykes, *Microstructural analysis of hydrogen absorption in 2NaH+MgB(2)*. Scripta Materialia, 2011. **64**(4): p. 351-354.
[27] Barkhordarian, G., T. Klassen, M. Dornheim, and R. Bormann, *Unexpected kinetic effect of MgB2 in reactive hydride composites containing complex borohydrides*. Journal of Alloys and Compounds, 2007. **440**(1–2): p. L18-L21.
[28] Pistidda, C., S. Garroni, C.B. Minella, F. Dolci, T.R. Jensen, P. Nolis, U. Bösenberg, Y. Cerenius, W. Lohstroh, M. Fichtner, M.D. Baro, R. Bormann, and M. Dornheim, *Pressure Effect on the 2NaH+MgB(2) Hydrogen Absorption Reaction*. Journal of Physical Chemistry C, 2010. **114**(49): p. 21816-21823.
[29] San-Martin, A. and F. Manchester, *The H-Na (Hydrogen-Sodium) system*. Journal of Phase Equilibria, 1990. **11**(3): p. 287-294.
[30] Stasinevich, D. and G. Egorenko, *Thermographic investigation of alkali metal and magnesium tetrahydroborates at pressures up to 10 atm*. Russ J Inorg Chem, 1968. **13**(3): p. 341-3.

Supporting Information

Title: Milling time effect of Reactive Hydride Composites of NaF-NaH-MgB_2 investigated by *in situ* powder diffraction

Authors: Michael Heere[1], Magnus H. Sørby[1], Claudio Pistidda[2], Martin Dornheim[2], Bjørn C. Hauback[1]

[1]Physics Department, Institute for Energy Technology, NO-2027 Kjeller, Norway

[2]Institute of Materials Research, Materials Technology, Helmholtz-Zentrum Geesthacht, D-21502 Geesthacht, Germany

Supporting information – S1

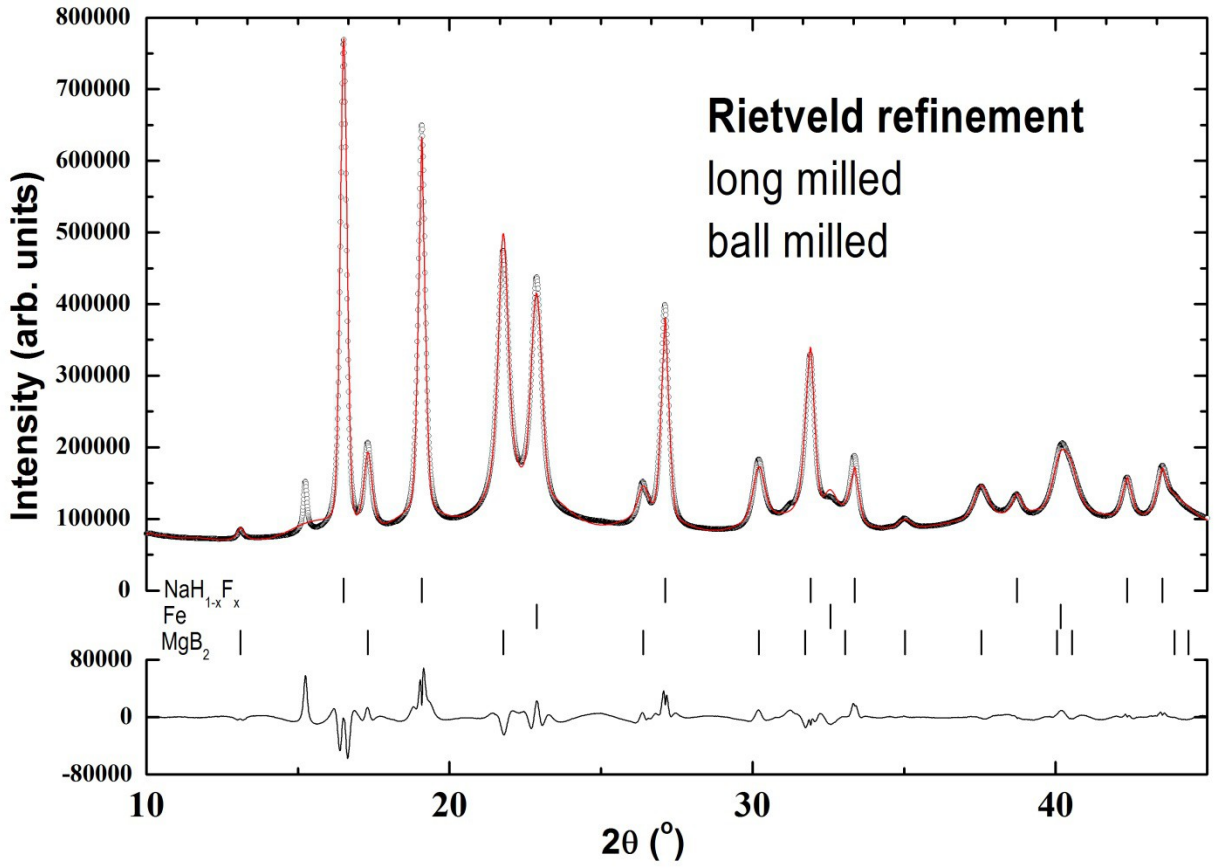

Fig. S1: Rietveld refinement plot from SR-PXD patterns at RT after ball milling showing experimental (circles) and calculated (red line) patterns, and a difference plot (below) for the long milled NaF+9NaH+5MgB_2. Vertical ticks mark the Bragg peak positions for (from top): $NaH_{1-x}F_x$ (51.2(3) wt%, x = 0.099(1)), Fe (4.3(1) wt%) and MgB_2 (44.5(2) wt %); R_{wp} = 4.43 %.

Supporting information – S2

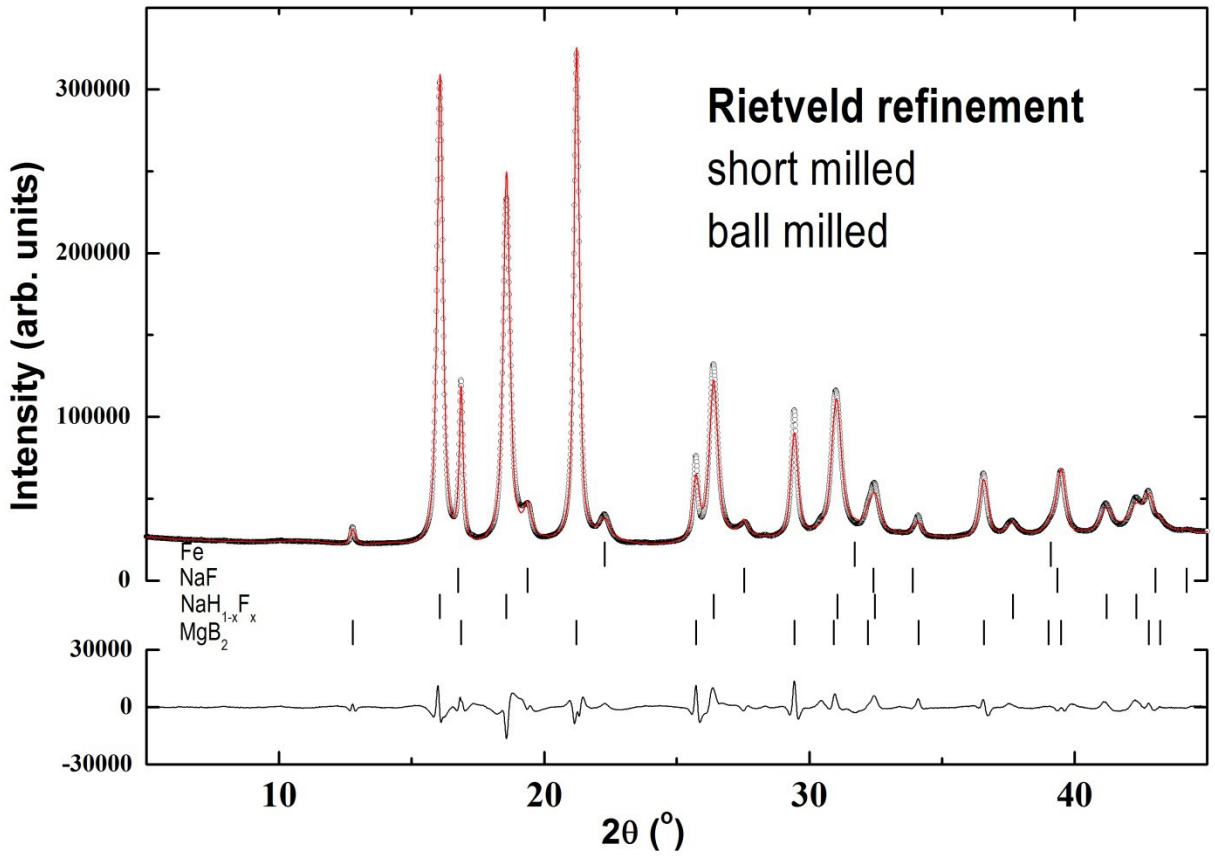

Fig. S2: Rietveld refinement plot from SR-PXD patterns at RT after ball milling showing experimental (circles) and calculated (red line) patterns, and a difference plot (below) for the short milled NaF+9NaH+5MgB_2. Vertical ticks mark the Bragg peak positions for (from top): Fe (0.5(1) wt%); NaF (2.9(3) wt%), $NaH_{1-x}F_x$ (59.6(6) wt%, x = 0.078(1) and MgB_2 (37.1(1) wt%); R_{wp} = 3.94 %.

Supporting information – S3

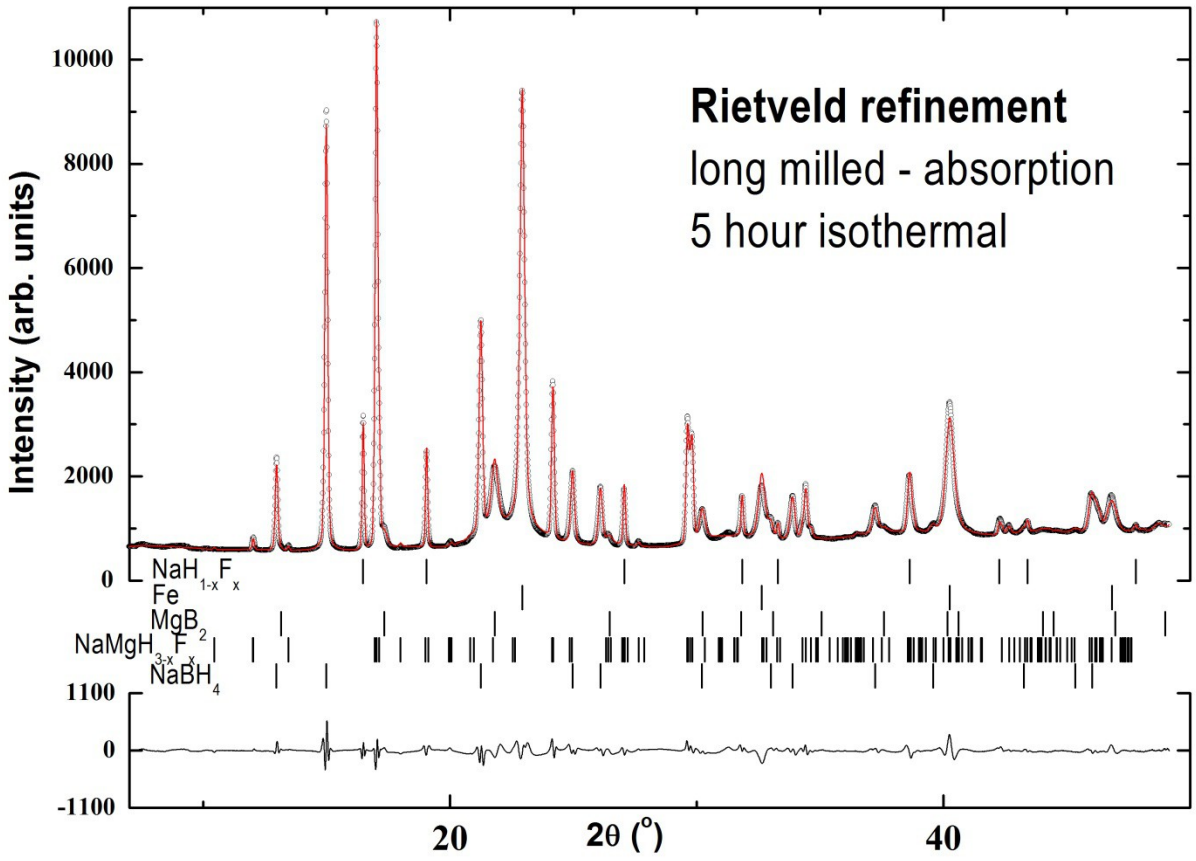

Fig. S3: Rietveld refinement plot from SR-PXD patterns at RT after 5 h isothermal hydrogenation at 325 °C showing experimental (circles) and calculated (red line) patterns, and a difference plot (below) for the long milled NaF+9NaH+5MgB₂. Vertical ticks mark the Bragg peak positions for (from top): $NaH_{1-x}F_x$ (6.9(1) wt%, x = 0.074(4)), Fe (9.2(1) wt%), MgB_2 (17.8(1) wt%), $NaMgH_{3-x}F_x$ (24.5(2) wt%, x = 0.848(3)) and $NaBH_4$ (41.5(2) wt%); R_{wp} = 3.73 %.

Supporting information – S4

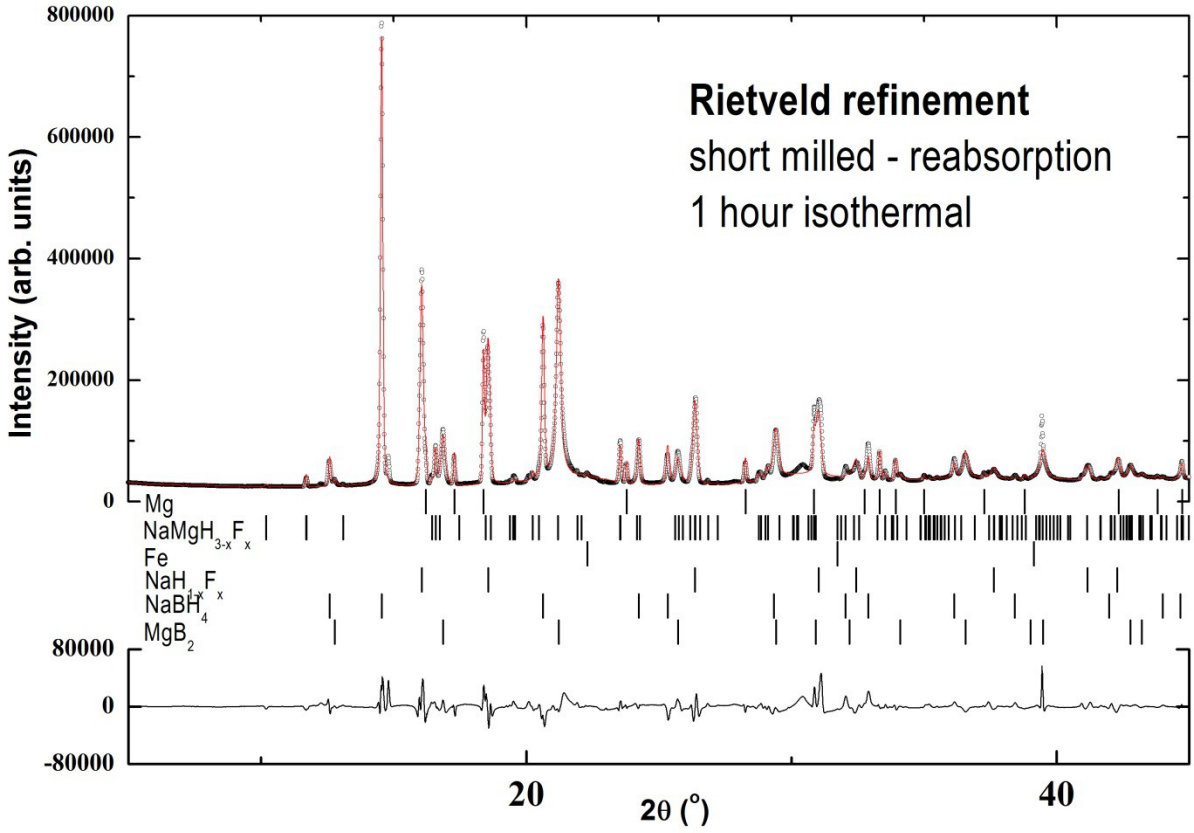

Fig. S4: Rietveld refinement plot from SR-PXD patterns at RT after 1 h isothermal re-absorption at 325 °C showing experimental (circles) and calculated (red line) patterns, and a difference plot (below) for the short milled NaF+9NaH+5MgB₂. Vertical ticks mark the Bragg peak positions for (from top): Mg (3.2(1) wt%), $NaMgH_{3-x}F_x$ (3.8(8) wt%, x = 1), Fe (0.038(7) wt%), $NaH_{1-x}F_x$ (14.5(1) wt%, x = 0.71), $NaBH_4$ (52.5(2) wt%) and MgB_2 (26.0(2) wt%); R_{wp} = 8.72 %.